Lighting Res. Technol. 2018; **0**: 1–21

Image-based perceptual analysis of lit environments

N Zhao PhD, **CF Reinhart** PhD and **JA Paradiso** PhD
MIT Media Lab, Cambridge, MA, USA

Received 2 April 2018; Revised 5 June 2018; Accepted 13 June 2018

Modern lighting systems typically provide a number of control parameters, e.g. colour and intensity, which allows nearly infinite possible configurations in one single room. The growing complexity of control makes it increasingly challenging for the user to configure the system and fully utilize the additional degrees of freedom. In contrast, an intuitive control interface takes into account the perceptual meaning of the lighting configurations. Unfortunately, collecting user ratings to construct perceptual models for lit spaces is cumbersome. To address this problem, we introduce an image-based mapping method that can rapidly evaluate the perceptual impression of lighting scenes using photographs or renderings. We discuss potential applications, guidelines and limitations of this method. In summary, we were able to closely approximate ratings-based mapping (normalized dissimilarity value <0.04). Among three dimensionality reduction methods, principal component analysis achieved the lowest dissimilarity and required the least images with a resolution as low as six by six pixels. Furthermore, simulations revealed that one perceptual model might suffice for the same type of offices. Offices of different types, on the other hand, require new mapping.

1. Introduction

With the advent of solid-state lighting, our ability to control artificial lighting for indoor illumination has substantially improved. LEDs can provide high dimming speed and dimming resolution, which is being explored in concepts such as visible light communication. They also enable high spatial resolution, e.g. for LED walls, displays and strips. Colour mixing using multiple emitters with different wavelengths permits the user to select from a palette of millions of colours.

These new degrees of control enable new experiences for indoor illumination. For example, in the office environment, we can dynamically introduce accent lighting to create a pleasant ambiance or adapt the lighting for various activities, for example work with displays, presentations, highly focused tasks, creative brainstorms, and restorative breaks. Numerous research projects have shown that different lighting conditions are required for different tasks.[1–3]

In order to advance new applications, we need to improve upon our current lighting control solutions. A lighting system with four solid-state luminaires, each with three colour channels (RGB) and 8-bit dimming resolution, can produce over a billion possible lighting compositions. The nearly infinite numbers of solutions make the complexity of control unacceptable for the end-user. Currently, preprogrammed lighting scenes are commonly used to improve usability. This approach reduces the number of lighting combinations to only a handful, restricting

Address for correspondence: Nan Zhao, MIT Media Lab, 75 Amherst Street, E14-548, Cambridge, MA 02139, USA.
E-mail: nanzhao@media.mit.edu

10.1177/1477153518786768

the richness of the system in favour of simplicity.

An approach that could preserve the richness while reducing the complexity is to discover a better representation of the control capabilities. In other words, instead of using a large set of device-centred control dimensions, e.g. dimmers for 8-bit RGB colour channels, we introduce a small set of abstract user-centred control dimensions that correspond to the user's perception, e.g. dimmers for focus and restoration. We also refer to this method as perceptual mapping and perceptual control for lighting.

A lighting system with 4 RGB-luminaires would need 12 device-centred control dimensions. These dimensions access the complete solution space. Using the perceptual control approach, we can compress the solution space to two or three abstract user-centred control dimensions that establish a new control map. The control map gives the user access to a continuous subset of the most interesting and relevant lighting configurations. We locate this subset using a very small number of *landmark lighting scenes*. Landmark lighting scenes are example scenes designed by a practitioner, the user or computer generated based on domain knowledge.

It is possible to discover latent dimensions for lighting control using user ratings of lighting scenes. In the past, researchers applied the semantic differential method[4] in combination with a mood board,[5] and observations[6] to collect data and construct latent models. Their work offered insight into human judgment of lighting[7] and lighting design.[8] More recently, researchers have demonstrated that the perceptual model could improve user interface design for lighting control[4] and for context-aware lighting.[9] Context-awareness is a form of computing that uses sensors and other inputs to infer the user's context, e.g. identity, location, and activities. Based on this information, the system automates control operations, for example to maximize energy savings and user comfort without burdening users with the additional control tasks. While it is also possible to use device-centred control dimensions for context-aware applications,[9–11] this approach is challenged by the curse of dimensionality, which means that when the number of control dimensions increase, e.g. by adding more colour channels and spatial resolution, the design of control rules becomes exponentially more complex. The perceptual control approach addresses this problem. It reduces the number of control dimensions in a meaningful way and simplifies the integration of sensing and lighting output. Therefore, this method has the potential to improve the usability of complex lighting systems and opens up possibilities for automation.

Using ratings to build perceptual models is limited due to observer fatigue. Moreover, collecting user ratings is time-consuming. In this paper, we introduce an image-based approach that can accelerate this process and rapidly construct a perceptual model. Images, such as photographs or simulations, have been proven to be useful for lighting evaluation and control.[12–16] Camera imaging has also been utilized for context-aware applications,[10,11,13] such as using images and quantitative features for daylight controls as well as tuning light levels based on user perception.

In our work, we use images to evaluate lighting scenes in order to establish a latent model that could describe the perceptual meaning of these scenes. The image-based model establishes a representation of the relative relationships of lighting scenes. We call this approach image-based mapping – a method for rapid computational analysis of lighting scenes. If the image-based map can approximate user ratings, then we can use only user ratings of a few scenes to label many scenes for perceptual control.

In this paper, we evaluate our method's ability to approximate user ratings and how

the image-based map generalizes for different variations of spaces. Little is understood how the perceptual controller generalizes for other spaces because previous research focused on a single space. This examination explores the generalizability of image-based mapping and perceptual lighting control. The outcome helps to prioritize future research in these areas.

In the first experiment, we evaluated the performance and limits of image-based mapping for approximating ratings. We computed two-dimensional representations of six lighting scenes using photographs of the experiment room – Lighting Lab – and compared the outcome to a representation derived from user ratings of the same space and lighting scenes. We introduced a dissimilarity measure, which is the basis of our evaluation. We examined three dimensionality reduction techniques for image-based mapping and different parameters for the image datasets, e.g. image resolution and angle of view.

In the second experiment, we explored the generalizability of the perceptual control approach. For this experiment, we created simulations of 16 different spaces and computed image-based mapping for each space. We compared their outcomes to examine whether the perceptual control map could be generalized within certain constraints for different types of spaces with different furniture and lighting. In the Applications and Outlook section, we offer our vision of potential applications for lighting design and control, and how this approach could improve today's practice.

2. Background

Flynn *et al.*[7] were pioneers in applying multivariate statistics to study the perception of lighting. The authors reasoned that environmental cues facilitated or altered through illumination should be measurable as a consistent change of impression under varying lighting conditions. They exposed study participants to six lighting scenes and asked them to rate the conditions using semantic differential scales, for example, spacious/cramped and sociable/unsociable. Applying factor analysis on the ratings, Flynn *et al.* found five perceptual factors that would explain the variance in impression and named them evaluative, perceptual clarity, spatial complexity, spaciousness and formality. This work has been influential for contemporary lighting research.[3] Other researchers discovered perceptual dimensions such as coziness/liveliness/tenseness[17] and activity/warmth/attention.[5]

Aldrich[4] introduced a lighting controller that was derived from user's perceptual ratings of lighting scenes. Using multivariate statistics and test subjects' aesthetic judgments of varying illumination settings in the same scene, he established two fundamental perceptual dimensions for the scene – colour temperature and appearance. A user interface based on these two degrees of freedom was more intuitive than a conventional, luminaire-by-luminaire control interface. Task fulfilment time was reduced to half. The new interface also allowed the user to access a wide range of lighting conditions, which is an improvement over preprogrammed lighting scenes.

Zhao *et al.*[9] identified control dimensions that correspond to the user's activities and derived a contextual two-dimensional – Focus and Casual – representation for a context-aware lighting controller in an office space. Using the focus/casual map, Zhao *et al.* achieved significant energy savings. Users reported that the lighting changes supported their tasks because the transitions were in accordance with their activities.

Quantification of perception can also be found in other domains of research, for example machine interpretation of music and music recommendation. Whitman[18] introduced an approach that links acoustic

analysis of musical compositions to manually drafted descriptions of meaning. The acoustic analysis does not directly provide the perceptual meaning of the music but reveals how different songs relate to each other. This is useful, for example, for classifying a large collection of music with only a small subset of labelled songs, which have manually drafted descriptions of meaning. Today, Whitman's work is used for music recommendation in a popular online radio application Spotify.[19]

Our approach for image analysis builds on a similar principle: the measurement of similarity of lighting scenes. The measurement of similarity relies on good visual features that contain the most relevant information in the image. Features could be edges, shapes, colours and other defining characteristics. Several feature detection methods such as linear and non-linear dimensionality reduction methods as well as other machine learning approaches and neural networks have been developed and constantly improved.

Dimensionality reduction methods are promising tools for the extraction of perceptual information in images. However, lighting artifacts are often an unwanted factor in image analysis for object recognition because changing lighting conditions complicate the prediction. For lighting applications, we need to identify features that specialize on extracting information about lighting and perception of rooms. In this paper, we evaluate three possible algorithms for image-based mapping.

Related research has considered lighting designs by optimising a perception-based image quality function.[20,21] The goal is to discover the best lighting configurations, for example, to maximize visibility of objects or scenes. In our work, we created the initial landmark lighting scenes in collaboration with a lighting designer. However, we can imagine a scenario that incorporates lighting optimization algorithms to assist the discovery of landmark lighting scenes in the future. The focus of this paper is image-based mapping of predefined lighting scenes and the evaluation of how this map differs from a model derived from user ratings and how it varies for different variations of spaces and interior design.

3. Image-based mapping

We used Radiance RGBE Encoding (.hdr) for the images. RGBE is an image format introduced by Ward and Simmons.[22] This encoding is an improvement over the RGB standard, both regarding precision and regarding dynamic range. Each colour channel – red, green, and blue – has the precision of 32 Bit floating-point values instead of 8 Bit in the standard RGB encoding.

We performed several processing steps to generate formatted datasets. First, we took into account the logarithmic relationship of human perception and stimulus intensity as stated in Fechner's Law[23] and used the logarithm of the weighted channel intensities. A small offset $offset = 0.1$ was empirically chosen and added to avoid $log(0)$. The following function was applied to each channel C.

$$C' = log((C + offset)) \tag{1}$$

We reshaped the processed pixel matrix ($height \times width \times 3$) to a vector ($1 \times (height \times width \times 3)$). The image vectors were concatenated to form an image data matrix ($number\ of\ images \times (height \times width \times 3)$). The labels of the images, which were the names of the respective lighting scenes, were stored in a separate vector ($1 \times number\ of\ images$). The order of the image vectors in the image data matrix and the associated labels in the label vector were jointly randomized. The randomized matrices together produced a formatted dataset.

The number of observations is the number of images in the dataset. Each observation contains $n = height \times width \times 3$ pixel values.

We performed dimensionality reduction on the dataset using the MATLAB toolbox for dimensionality reduction by Van der Maaten[24] with target dimensionality of two and visualized the landmark lighting scenes in the resulting representation. We considered several dimensionality reduction techniques for image-based mapping, which are discussed further below.

Advanced machine learning techniques, such as dimensionality reduction techniques, are used to analyse underlying structures – embeddings – in datasets. They have demonstrated outstanding performance in extracting features in images. Dimensionality reduction is also used for data visualization, where high dimensional data are organized into a two-dimensional space for graphical display (see Van der Maaten[24] for further information on dimensionality reduction).

4. Definition of dissimilarity

In order to compare image-based and rating-based representations, we computed a dissimilarity value

$$D = e(S_{Img},\ S_{Rate}) \tag{2}$$

This measure of error indicates the difference between two two-dimensional representations of lighting scenes. A linear transformation is first applied to align the two representations and the error is computed based on the remaining distances of the landmark lighting scenes. In other words, this measure evaluates the dissimilarity of the relative positions of the landmark lighting scenes. We did not consider the linear transformation as an error itself. In the Applications and Outlook section, we talk more about potential solutions to transform the image-based mapping results to align with predefined axes.

A dissimilarity value of 0.09 and 0.04 means, for example, that the coordinates of the landmark lighting scenes in the first representation are shifted by 30% and 20%, respectively, in the second representation. We choose $D = 0.09$ to be the threshold of an acceptable dissimilarity value. This threshold should be reviewed in the future because the requirement for precision might change depending on the desired application. The dissimilarity value is useful for relative comparison and could become a benchmark value.

First, we calculated the centroid of the lighting scenes for both two-dimensional representations using

$$[C_x, C_y] = \left[\frac{1}{N}\sum_{j=1}^{N} S_{j,x},\ \frac{1}{N}\sum_{j=1}^{N} S_{j,y}\right] = [\bar{S}_x, \bar{S}_y] \tag{3}$$

where N is the number of scenes and $S_j = [S_{j,x}\ ,\ S_{j,y}]$ is the x,y-coordinates of the j-th scene in the two-dimensional representation. We applied an offset to the two-dimensional map so that the centroid became the origin. We then normalized the map so that the coordinates of the landmark lighting scenes were between -1 and 1. This was achieved by dividing the x,y-coordinates with the maximum x- and y-value, respectively.

Next, we performed procrustes analysis[25] on the normalized image- and rating-derived representations S'_{Img} and S'_{Rate} to determine the linear transformation that would align the two representations. Finally, the dissimilarity value D is the sum of squared errors of the transformed landmarks S''_{Img}, standardized by a measure of the scale of S'_{Rate}

$$D = \frac{\sum_{d=1}^{2}\sum_{j=1}^{N}(S'_{Rate,j,d} - S''_{Img,j,d})^2}{\sum_{d=1}^{2}\sum_{j=1}^{N}(S'_{Rate,j,d})^2} \tag{4}$$

5. Experiment 1

In the first experiment, we examined whether image-based mapping can approximate rating-based mapping of lighting scenes. We took photographs of six preset landmark lighting scenes in the Lighting Lab and applied image-based mapping using three dimensionality reduction techniques: a linear technique (PCA), a non-linear technique (Isomap), and a technique (t-SNE) that is especially useful for data visualization. They were chosen for their respective properties. Furthermore, we generated several datasets by varying parameters such as sample size, image resolution, angle and field of view and dynamic range. To examine the effects of these parameters, we applied image-based mapping for each variation using PCA. PCA was selected because it was established as the most suitable technique in the before-mentioned comparison of dimensionality reduction methods.

We compared image-based mapping results to a rating-based map that was established in a prior study from user ratings of the same lighting scenes in the Lighting Lab. The dissimilarity of the image- and rating-based representations as defined above was the basis of our evaluation.

5.1 The Lighting Lab

The Lighting Lab is a windowless office (4.2 m in length, 2.8 m in width, and ceiling height of 2.6 m) with two tables in the centre and chairs along their edges facing each other. The table height was 0.7 m. There were books, objects, sketching paper, pens, an office phone, a mug, a laptop computer and some other office supplies on the table. Additionally, there were three decorative paintings on the walls and a white file cabinet with books.

The lighting installation consisted of six 5-channel wall washing luminaires (Philips Color Kinetics SkyRibbon IntelliHue Wall Washing Powercore) with dimensions $0.56\,\text{m} \times 0.10\,\text{m}$ and two 5-channel recessed downlights (Philips Color Kinetics SkyRibbon IntelliHue Linear Direct Powercore) with dimensions $1.2\,\text{m} \times 0.10\,\text{m}$. The light luminaires were divided into six lighting groups as illustrated in Figure 1.

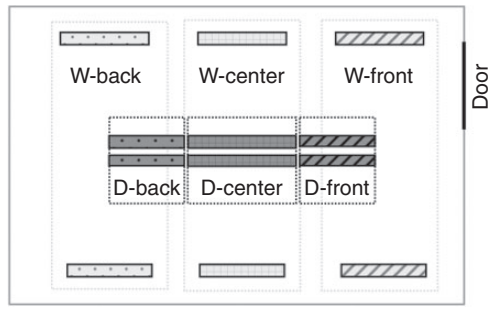

Figure 1 Lighting setup and grouping illustrated by the dashed outlines and hatching. In the centre are downlight luminaires (D) and along the walls are wall-washing luminaires (W)

5.2 Lighting scenes

Six landmark lighting scenes were created in collaboration with a lighting designer for the Lighting Lab. The settings of the lighting scenes are detailed in Table 1. Figure 2 shows photographs of the scenes.

5.3 User ratings

Ratings of user perception for the six lighting scenes in the Lighting Lab were collected and analysed in a previous study.[9]

Participants ($N = 17$, from 20 to 35 years old) rated the suitability of lighting scenes for 14 office tasks. They recorded their opinions on a five-point Likert scale from strongly disagree to strongly agree, including an option to give no answer. Each participant rated all conditions in random order. The office tasks in the questionnaire were chosen according to guesses of potentially relevant contextual dimensions in the office. The tasks were:

- casual conversation with a friend
- informal phone conversation

Table 1 Lighting configurations, light output and colour

Light group	Scene 1	Scene 2	Scene 3	Scene 4	Scene 5	Scene 6
Percentage of maximum light output						
W-back	–	90%	–	90%	20%	–
W-cent.	–	90%	90%	90%	20%	–
W-front	–	90%	–	90%	20%	40%
D-back	60%	4%	–	65%	100%	–
D-cent.	60%	4%	65%	65%	100%	–
D-front	60%	4%	–	65%	100%	40%
Colour temperature in degrees Kelvin						
All	3000	3000	3000	6500	6500	3000

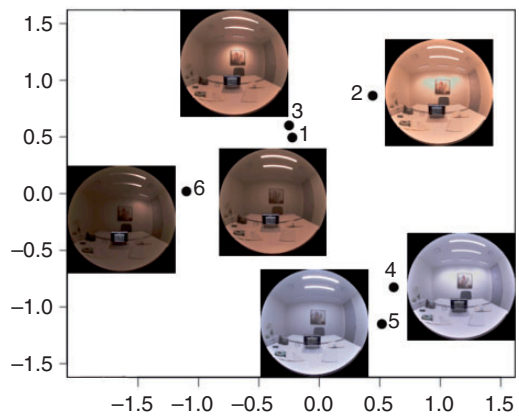

Figure 2 Results from the user ratings. The lighting scenes are visualized according to the first two rotated principal components

- coffee break
- sketching on paper
- study/memorization
- hand-craft
- formal phone conversation
- brainstorming in a group
- programming/CAD or video editing on a computer
- informal presentation with slides
- creative task using a computer
- (routine) email on computer
- formal presentation with slides
- formal phone conversation.

PCA was applied to discover latent dimensions of user judgment. This analysis was performed using the PSYCH package in R[26] and the Varimax rotation method.[27] The data were formatted in a way that each observation contained ratings for all questions of one subject for one lighting scene.

Figure 2 shows the resulting two-dimensional perceptual representation that was established using the first two rotated components. The average component scores of each lighting scene determined their coordinates in this representation. The first two components were named focus and casual because focused activities (e.g. sketching on paper, study/memorization, formal phone conversation) loaded with the first component and casual activities (e.g. casual conversation with a friend, informal phone conversation, coffee break) loaded with the second component. Focus configurations used more uniform and brighter lighting, whereas casual configurations used lighting with warm colour temperature. Zhao *et al.*[9] gives a more detailed discussion of these results.

In the following, we refer to this representation as the rating-based map. We use the rating-based map as a basis for the evaluation of image-based perceptual analysis.

5.4 Photography

We used a DSLR camera (Canon, Canon D5) with an ultra-wide-angle lens. The camera was equipped with an HDR capable firmware,[28] which we used to take HDR photographs. In the firmware settings,

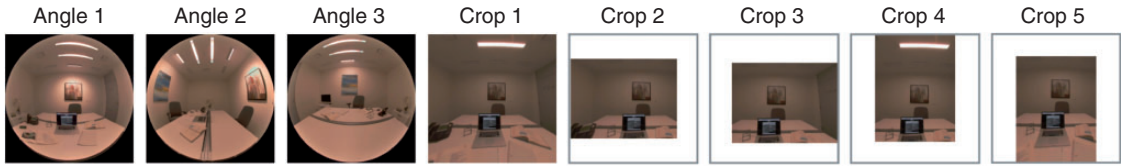

Figure 3 Angles of view used for comparison

we configured the camera to use nine brackets and two exposure value (EV) increments, which means that for each HDR photograph, the camera took nine images and after each image, the exposure was increased by two stops. A two stop increase is, for example, a change in shutter speed from 1/8 of a second to 1/2 of a second, from 1/2 of a second to 2 s, and so on. ISO and white balance settings were fixed to 100 and daylight, respectively. The image resolution was 5616 by 3744 pixels.

HDR images were computed using nine photographs for each image, and the Photosphere command line tool.[29] We provided the software with a calibration file, which was generated using our camera setup and a luminance meter. The calibration file was created from manual calibration in Photosphere. The output HDR images were stored with the Radiance RGBE Encoding. In a post-processing step, the images were centred, cropped and re-sized to 512 by 512 pixels. We measured a vignetting function for the camera lens and applied it to the images.[14] We applied an intensity scale factor based on readings from the luminance meter to convert pixel values to units of $Wsr^{-1}m^{-2}$ .We converted from luminance to radiance units because analysis software, for example software that performs glare assessment, expects radiometric input.[30] Figure 2 shows the images after post processing.

5.5 Dimensionality reduction methods

We considered three dimensionality reduction techniques: PCA, Isomap and t-SNE.

Principal component analysis (PCA) is a linear dimensionality reduction method, which computes a lower dimensional subspace in which the variance of the data is maximal. PCA is a popular algorithm commonly used for face recognition and feature detection in machine learning applications. One characteristic of this method is that it focuses on preserving the global structure of the data, meaning the large pairwise distances between samples and is less effective at conserving local structures, keeping samples with small pairwise distances close together.[31]

Isomap, on the other hand, aims to preserve local structures by retaining the geodesic rather than the Euclidean distance between data points. The geodesic distance is measured over the manifold on which the data points lie. It is the shortest path between two points in a neighbourhood graph.[31]

Lastly, t-SNE was developed to visualize data that lie on several related manifolds, such as images of objects, which, for example, could be grouped by colour and the shape of the objects. This algorithm can reveal both a global and local structure in the data at several scales.[32] A quality of this algorithm is that it models dissimilar data points using large pairwise distances, and models similar data points using small pairwise distances, which results in well-separated clusters for data visualization.

For the comparison of dimensionality reduction methods, we created an image dataset using photographs of the six landmark lighting scenes (Angle 1, see Figure 3) and supplemental images with 100 interpolation steps, which generated a final sample size of 1491 images. Supplemental images were linear combinations of the original

images. For each step, the multiplicative weight of one image was increased, and the other was decreased. The supplemental images artificially inflated the sample size. They showed new lighting conditions created using two lighting scenes. We reduced the resolution of the photographs from 512 by 512 to 52 by 52 pixels using a bicubic interpolation algorithm to accelerate computation.

5.6 Parameters

We generated several datasets by varying the number of images, image resolution, angle and field of view and dynamic range.

5.6.1 Number of images

We generated five collections of images with different total numbers of supplemental images from 0 to 100 interpolation steps between unique pairs of lighting scenes. Image resolution (52 by 52), angle of view (Angle 1, see Figure 3) and encoding (HDR) were the same for all images.

5.6.2 Image resolution

We examined the effect of image resolution using eight collections of images with resolutions ranging from 1 by 1 to 512 by 512 pixels; 512 by 512 HDR images were resized using a bicubic interpolation algorithm to create lower resolution images. Angle of view (Angle 1, see Figure 3) and encoding (HDR) were the same for all images and no supplemental images were added to the datasets.

5.6.3 Angle and field of view

The human field of vision is limited, so is the field of view of most types of cameras. One would need to decide the position and orientation of the camera to collect sample photographs. What angle of view is the most suitable for the analysis of interior lighting? To address this question, we generated datasets using three different camera positions and five uniquely cropped images. We took photographs from three positions using the wide-angle lens: an overview position that showed both workstations at the shared table and two different seated positions on each side of the table. For the cropped images, we generated pictures with a narrower view by cropping 20% along different edges of the undistorted photographs. We used the MATLAB Camera Calibration App[33] to create a custom calibration file for the wide-angle lens and to undistort the original photographs. Figure 3 presents the photographs from the three camera positions and the undistorted, cropped images. Image resolution (52 by 52 pixels) and encoding (HDR) were constant for all images. No supplemental images were added.

5.6.4 Dynamic range

We analysed how HDR images compared to 8-Bit RGB encoded images. We used five collections of images. The first one contained HDR photographs. For the other four, we generated JPEG images with four different exposure levels from the HDR photographs using Radiance, a lighting simulation and rendering software.[34] We added supplemental images with 50 interpolation steps to visualize the distortion caused by the saturated pixels. All images used the same angle of view (Angle 1) and had a resolution of 52 by 52 pixels.

6. Experiment 1: Results and discussion

The analysis using photographs established a lower dimensional representation that was a close approximation ($D < 0.04$) of the rating-based representation. The settings that led to this result are shown in Table 2. The angle of view, Angle 3, corresponds to where the participants were positioned in the Lighting Lab during the user-rating experiment. Among the three dimensionality reduction methods, PCA achieved the lowest

dissimilarity value. A linear transformation (e.g. translation and orthogonal rotation) was necessary to align the principal components with the rating-based map. However, after a simple transformation, the rating- and image-based representations exhibited obvious similarities (see Figure 4). This outcome demonstrates that it is possible to approximate human judgment of perceptual differences of lighting scenes with the analysis of photographs of the lighting scenes. The following paragraphs discuss how different dimensionality reduction methods and parameters of the dataset affected the outcome.

Table 2 Using these parameters we achieved the lowest dissimilarity value D = 0.0396

Dimensionality reduction technique	Principal component analysis
Number of Images	6 images of the 6 landmark lighting scenes
Image resolution.	52 by 52 Pixels
Angle of view	Angle 3 (see Figure 3)
Dynamic range	HDR (.hdr)

6.1 Comparison of dimensionality reduction methods

Figure 4 shows the side-by-side comparisons of the image- and rating-based maps for all three dimensionality reduction methods. PCA achieved the lowest dissimilarity value (D = 0.093). The rating- and image-based representations exhibited obvious similarities. One remaining difference was the relative distance between scene 1 and scene 3. These two scenes were considered alike when rated according to their suitability for different work tasks, but the photographs of these scenes were comparatively distinct.

Isomap performed nearly as well as PCA (D = 0.110). The relative positions of the landmark lighting scenes were similar to the PCA result and the rating-based representation. The interpolated samples formed a nonlinear pattern showing the approximated geodesic distance between samples. In contrast, for PCA, the interpolated samples formed slightly curved lines between the landmark lighting scenes. Curved instead of straight lines were to be expected because pixel intensity is scaled logarithmically,

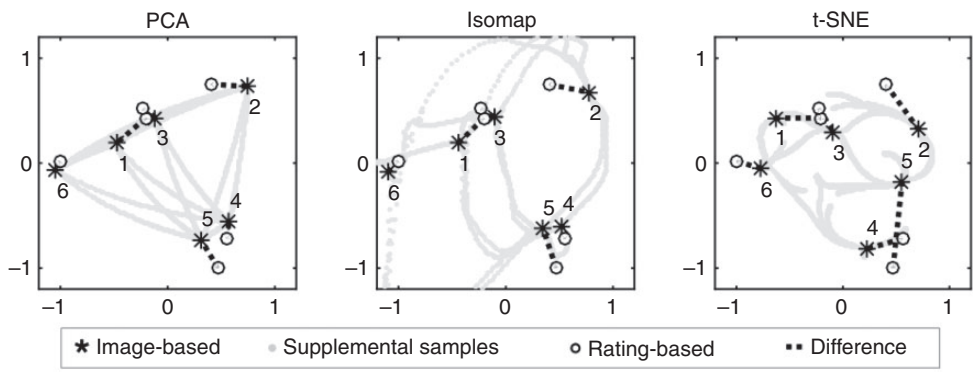

Figure 4 Comparison of three dimensionality reduction methods: PCA, Isomap and t-SNE. Each method was applied to a dataset of 1491, 52 by 52 HDR images of the Lighting Lab. The star-shaped markers show the position of the six lighting scenes on the image-based representation. The circle-shaped markers show the corresponding positions on the rating-based map. The black dashed line that connects the markers illustrates the difference between the rating-based and image-based results. The dot-shaped light grey markers represent the position of the supplemental images generated from interpolations of the six lighting scenes in the image-based map

whereas the supplemental images were generated with linear interpolation steps.

Lastly, the t-SNE produced the most distinct map ($D = 0.322$). Using this algorithm, the distant data points were positioned with large distances between each other. Therefore, on the 2D projection, each landmark lighting scene became an intersection of several sequences of samples. Landmark scenes formed independent islands surrounded by their closest variations.

The comparison revealed that PCA is the most suitable algorithm for image-based mapping for our choice of landmark lighting scenes. Given that PCA performed best, we can conclude that the latent structure can be discovered on basis of the distant samples, which were the landmark lighting scenes. This is further confirmed by the comparison of number of images.

The linear dimensionality technique was sufficient to discover the manifold or subspace of the solution space that was determined by the landmark lighting scenes. This means that this result is linked to our choice of lighting scenes, which we created by varying brightness, colour temperature and uniformity of six individually controllable luminaire groups. The number of design parameters is relatively low. Therefore, we were able to visualize them on a two-dimensional map using the linear technique. Results from the comparison of image resolution give further insights into the influence of these design parameters and are discussed below. These findings suggest that if similar design choices are made for the landmark lighting scenes, PCA should be the preferred method for dimensionality reduction.

If landmark lighting scenes were created using saturated colours and more spotlights in addition to our current choices, we believe that t-SNE could be a better method, because, in that case, more lighting design dimensions have to be compressed to the two-dimensional representation. t-SNE has been proven to be more suitable for data visualisation of high-dimensional data. If more complex design parameters are used, we also need to review our measure of dissimilarity for evaluation. Instead of comparing the two-dimensional representations, we could examine the number and relative positions of clusters in the map.

Isomap performed very similar to PCA; however, Isomap is more computationally intensive. The comparison of number of images confirms that PCA is the preferred choice over Isomap for its simplicity.

6.2 Number of images

When using PCA, the supplemental images did not increase the similarity to the rating-based representation (Figure 5). This outcome was plausible because the most distinct samples, the landmark lighting scenes, were also the most influential samples for PCA. In this specific case, the supplemental images decreased similarity, due to the additional information in the dataset. The result is sensitive to the interpolation method that we used to generate the supplemental images. Ideally, we would take additional photographs of the lit space instead of generating supplemental images.

As a follow-up analysis, we performed the same comparison using Isomap for dimensionality reduction. This comparison revealed the importance of the supplemental samples for this method (Figure 5). Given that Isomap preserves local structures, the supplemental images were necessary and dissimilarity value increased with decreasing sample size. PCA is the preferred method, because it only requires six images of the six landmark lighting scenes for the analysis.

6.3 Image resolution

Figure 6 shows that the dissimilarity value increases with decreasing resolution. Image resolution as low as 6 by 6 pixels was sufficient to preserve the information in the

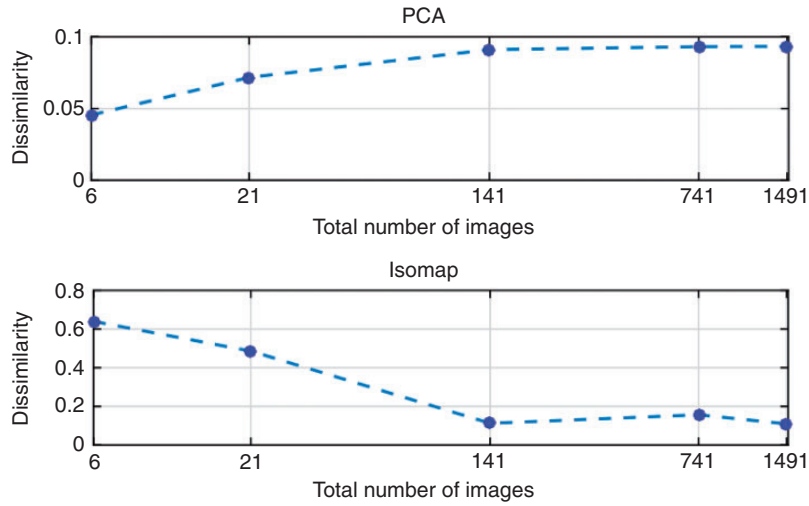

Figure 5 Comparison of datasets with different total numbers of images using PCA (top) and Isomap (bottom)

image. This outcome suggests that image-based mapping with PCA takes luminous distribution into account in addition to brightness and colour temperature of the lighting scenes. Brightness and colour temperature could be expressed in a single pixel. However, 6 by 6 pixel images contain information of brightness levels on large horizontal and vertical surfaces as well as location. This outcome reflects our choice of landmark lighting scenes, which we created by varying brightness, colour temperature and uniformity using six individually controllable luminaire groups.

Using low-resolution images could further increase computation speed and is preferred. However, the target resolution should match the complexity of lighting design and lighting effects. For example, the resolution should be increased to ensure a relevant result in an application in which there are more local contrasts than uniform luminance on the walls and large surfaces.

6.4 Angle and field of view

The outcome of this experiment indicated that the choice of camera view should be similar to the first person view of the worker. This means that the images should show the scene from a position where the worker sits or from a position where the worker is most likely to view the scene. Among the three different camera positions, the dissimilarity value was the lowest for Angle 3 (see Figure 3). Interestingly, Angle 3 was the same position where the study participants sat during the human subject study. This relation might have contributed to the increased similarity with the rating-based result. The photographs taken from this angle were a better representation of the participants' experience than the other camera angles. This angle showed a unique painting, which was illuminated differently than the painting visible from the other seated desk position (Angle 1). A filter attached to the wall-washing luminaire created a soft rather than hard spotlight on the painting. The dissimilarity value of the desk position (Angle 1) was lower than the overview position (Angle 2). Similarly, among the cropped images, the picture that best reflected the study participant's view, Crop 1 followed by Crop 5, achieved the lowest dissimilarity value.

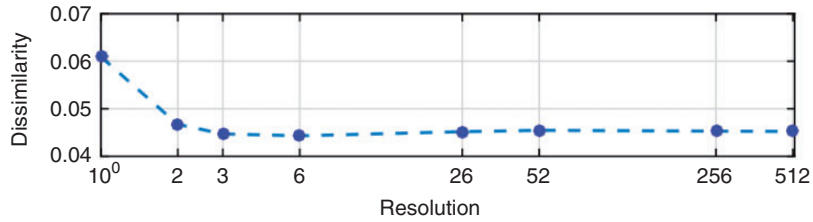

Figure 6 Comparison of image resolution

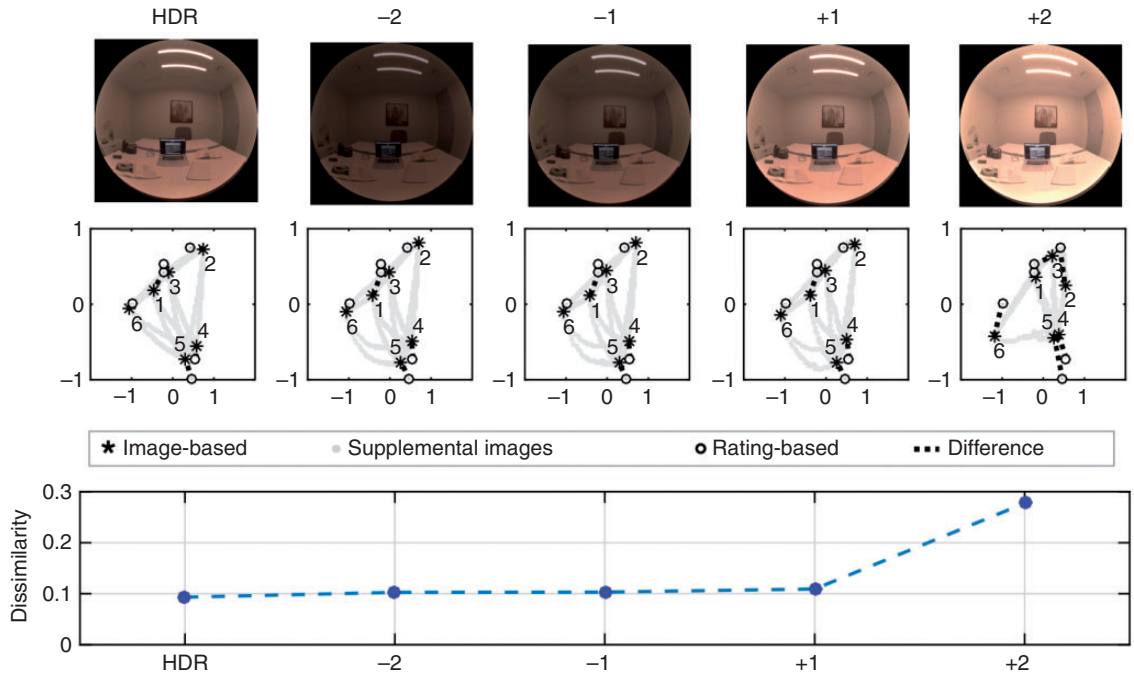

Figure 7 HDR images compared to 8-Bit RGB encoded images with different exposure level. The middle row shows the resulting maps using PCA. The bottom graph shows the corresponding dissimilarity values

6.5 Dynamic range

As shown in Figure 7, the HDR dataset achieved the lowest dissimilarity value and dissimilarity was lower for underexposure than overexposure. Underexposure is therefore recommended if the standard 8-Bit RGB encoding is used instead of HDR. Among the tested parameters for mapping using PCA, the dynamic range is the most impacting parameter and should be set with care according to the design.

7. Experiment 2

In the second experiment, we investigated how the perceptual control map can be generalized for other kinds of spaces.

For this experiment, we created simulated spaces with different space types, furniture and lighting setups. We compared image-based mapping of these spaces to each other and to the rating-based result. This time, we did not vary parameters for data acquisition and dimensionality reduction. We used PCA for dimensionality reduction, image resolution of 52 by 52, HDR encoding and 50 supplemental images for visualisation.

7.1 Spaces

For 3D rendering of simulated offices, we chose three types of spaces: a one-person office, a conference room and a small office. The one-person office has the smallest footprint. It is a private space that allows one person to work comfortably. The small office is a slightly bigger room that could facilitate two people. This space could be used for one-on-one meetings and collaborative work. The conference room is a large room that could host a group of people for meetings, presentations, group discussions, etc.

In order to build examples of the three types of spaces, we collaborated with Steelcase, a leading company for office furniture and interior architecture based in the USA. Steelcase created 3D models of the three types of offices. They created three variations for each type. The variations were windowless, with window and lounge setting. The lounge setting was furnished with a couch and coffee table instead of a work desk. These models comprised Steelcase's furniture, accessories and space division products.

Next, we added a ceiling lighting system to these spaces. The lighting system was modelled after the system in the Lighting Lab, which was used for the collection of user ratings. The position and quantity of lighting luminaires were adapted for each type of simulated space to fit the room size. As a constraint, the distance between the wall-washing luminaires was constant and the downlighting luminaires were always grouped as two continuous strips.

For the one-person office (see Figure 8(1)–(6)), we reduced the number of luminaires to adapt to its small footprint. We used four wall-washing and six downlighting luminaires instead of six wall-washing luminaires and eight downlighting luminaires as were originally installed in the Lighting Lab.

The small offices (see Figure 8(11)–(16)) were the most alike to the Lighting Lab in size and shape. Hence, we were able to use the same number of luminaires as the original setup in the Lighting Lab.

For the conference rooms (see Figure 8(7)–(10)), we added eight downlighting luminaires to the existing eight and doubled the output capacity of the wall-washing luminaires in Spaces 8–10 to compensate for the size of the room.

Figure 9 shows the layouts of the resulting lighting installations. By altering the layout of the lighting installation, we created 16 simulated offices based on the 9 variations of spaces as shown in Figure 8. There are one or two lighting installation layouts per variation of spaces.

7.2 Lighting scenes

The six landmark lighting scenes were similar to the ones used in the Lighting Lab. We adapted them according to the new layout of the lighting installation.

We made two changes for one-person offices to accommodate the new lighting layout and the small space. For scene 3, the gallery lighting scene, which formally used a combination of two wall-washing spotlights and four downlights, was reduced to only using two downlights to achieve a similar effect. Scene 6, the low light presentation mode, which previously used two wall-washing luminaires and two downlights, was reduced to only two wall-washing luminaires

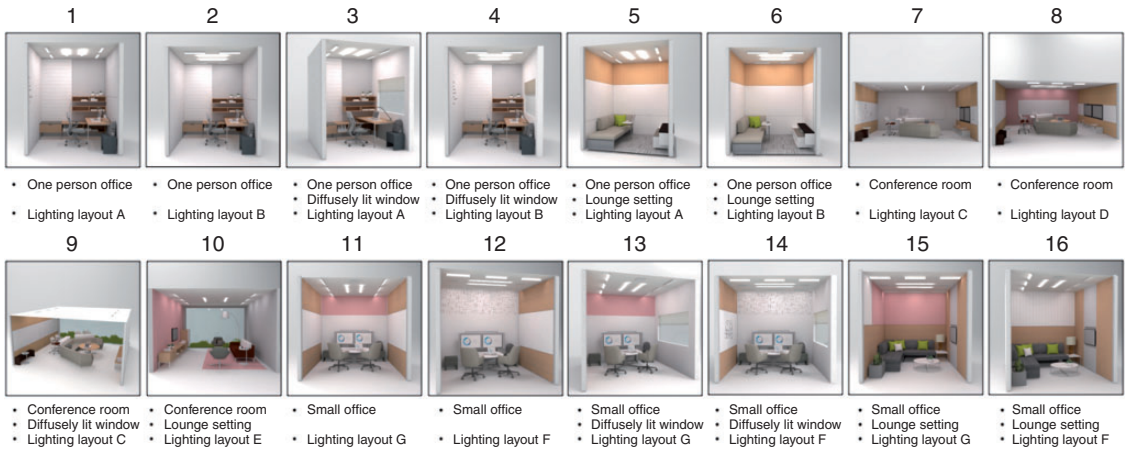

Figure 8 Renderings of the variations of simulated offices. One wall was removed to make the inside visible. The number on top of each image identifies the room

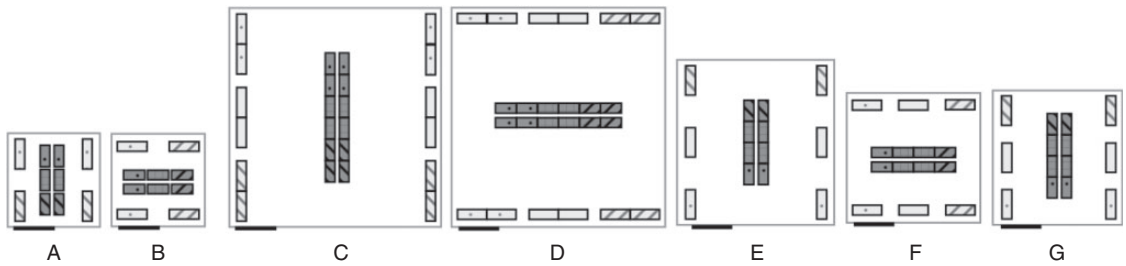

Figure 9 Layouts of lighting installation used for the simulated offices. The size of the diagram is an approximation to the corresponding size of the room. Both downlighting and wall-washing luminaires are divided into sections. The hatching represents their corresponding lighting (control) group

and half of the light output to achieve a similar effect.

For Scene 6, we positioned the light always on the opposite side of the viewing direction. This means that we used different luminaire to illuminate Scene 6 depending on the layout of the lighting installation.

We did not alter the lighting scenes for the small offices and for the conference rooms. However, as mentioned before, the light output was doubled for the large conference rooms. As an example, Figure 10 shows the six lighting scenes for the conference room with a diffusely lit window (Space 9).

7.3 3D rendering

HDR renderings were created using the 3D Rendering and Animation Software KeyShot.[35] Keyshot is a commercial software for 3D rendering and animation which has been suggested as an educational tool by Santamaría-Peña *et al.*[36] and has been used to render architectural interiors. This software uses a ray tracing technique to simulate global

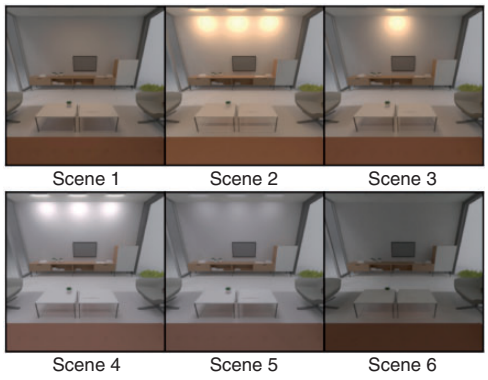

Figure 10 Renderings of the six lighting scenes for the simulated space 9

illumination (direct and indirect illumination) and supports HDR outputs. It provides a range of tunable material parameters, e.g. diffuse, specular, reflection, and roughness. It offers several illumination textures, e.g. diffused area lights, point lights and IES profiles. We used the diffused area light texture and configured them by specifying the colour temperature and light output in lumens. The maximum light output of each section of the downlighting luminaires, as illustrated in Figure 9, was set to be 800 lumens. The maximum of each section of the wall-washing luminaires, as illustrated in Figure 9, was set to be 2000 lumens.

8. Experiment 2: Results and discussion

The simulation results indicated that modification of interior attributes in large spaces (conference room and small office) created a greater variance in mapping outcome than in small spaces (one-person office). There were also more differences in mapping outcome among the three types of rooms than within the variations of one type (Figure 11).

We compared the imaged-based maps of the three types of spaces with the rating-based map to examine the generalisability of the Lighting Lab results.

The resulting maps for the six one-person offices (spaces 1 to 6, see Figure 11(1)–(6) in comparison to Figure 2) were skewed in comparison to the rating-based map ($D < 0.1643$). The relative distance between scene 6 to scene 3 and scene 1 was smaller in all versions of the one-person office than in the rating-based map (Figure 2). This outcome indicated that scene 6 created a dim diffused effect similar to scene 3 and scene 1, despite using half of the light output from the original design. Furthermore, scene 3 became more similar to scene 6 than scene 2 because we removed the wall-washing spotlights.

The maps of the small offices were the most similar to the rating-based map ($D < 0.1363$). The size of the small offices and the lighting layout were the most similar to the Lighting Lab. Consistent with this finding, the resulting maps for the conference rooms, which were the most distinct from the Lighting Lab, were also the most distinct from the rating-based map ($D < 0.2381$).

For each space type, we calculated the dissimilarity value for each variation in comparison to the windowless version to examine how the modification of furniture, lighting layout and diffusely lit window influenced the resulting maps. For one-person offices, conference rooms and small offices, the windowless versions were called spaces 1, 7, and 11, respectively.

Among the three types of spaces, the maps of the one-person offices 1 to 6 in Figure 11 were the least different from the windowless version ($D < 0.0041$). We can reason that because this type of office has a small footprint, light can bounce off nearby wall surfaces and create a uniform diffused illumination with little contrast. Therefore, the position of luminaires and the interior attributes had diminished impact on the resulting effect.

For the conference rooms, because of the large footprint, despite the increase in brightness and the number of light sources, the system produced high contrast and spotty

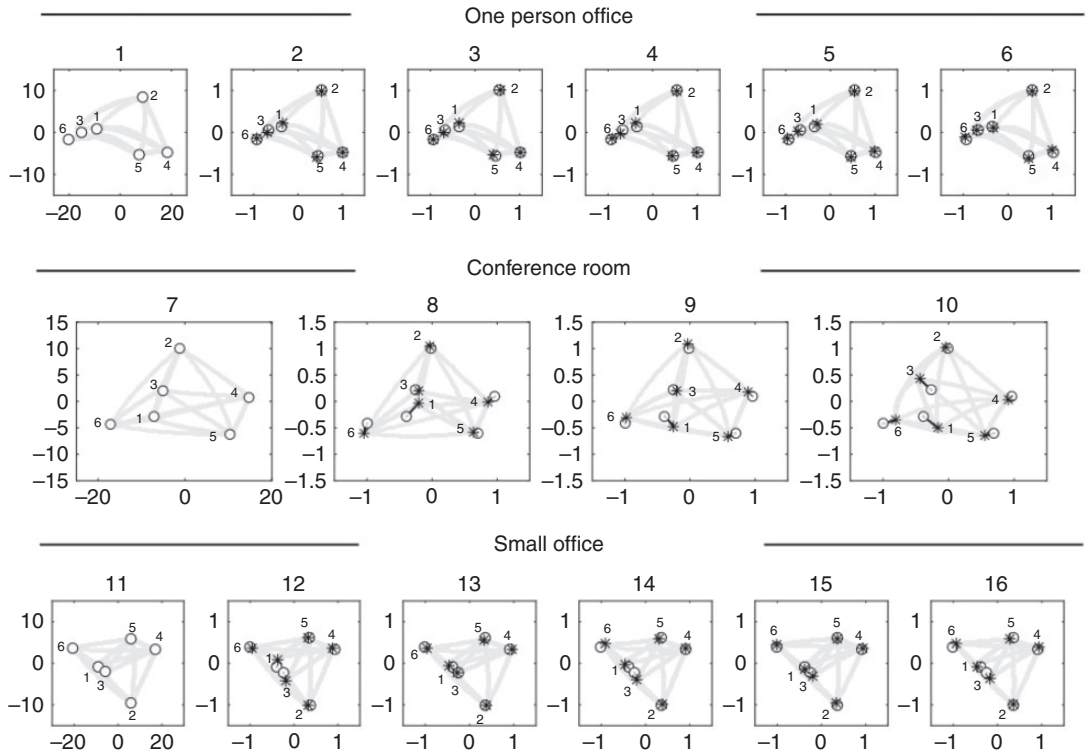

Figure 11 Results of the rendered images. Each diagram shows the resulting map of the simulated office with the corresponding number. The first map in each row (Nr. 1, 7, 11 with circle-shaped markers) is the windowless version of each office type, which was used as a reference for within-type comparison. In the remaining maps, the offsets between the reference map (circle-shaped markers) and the result (star-shaped marker) visualize the differences introduced by the variations of the lighting layout, furniture, and window

illumination patterns in the space. Among the variations, the lounge setting (Nr. 10) caused the greatest difference, larger than the diffusely lit window (Nr. 9). The different variations of conference rooms generated more distinct maps than the one-person offices ($D < 0.0582$).

The comparison of the variations of small offices (see Figure 11(11)–(16)) showed that the modification of lighting system layouts (Nr. 12, 14, 16) caused larger divergence than a diffusely lit window or change of furniture (Nr. 13 and 15) ($D < 0.0201$).

The outcome of this experiment suggests that the perceptual control map could be generalized for spaces of the same type. Change of lighting layout, furniture and the addition of a diffusely lit window had little impact ($D < 0.0582$) on the mapping outcome. Also, the comparison between the rating-based result of the Lighting Lab and the Small office confirmed that the similarity of these two spaces let to a rather low dissimilarity value of the derived maps ($D < 0.1363$).

The result of the conference rooms was the most distinct from the rating-based map of the Lighting Lab ($D < 0.2381$). Given the lack of generalisability from the Lighting Lab to conference rooms, further studies should be conducted to collect user ratings of conference room type spaces to evaluate the image and rating-based mapping approaches. The dissimilarity values among the variations of the conference rooms were small ($D < 0.0582$)

suggesting that maps for this type of space might be generalisable if a similar lighting setup and lighting scenes are used.

9. Applications and outlook

We envision this approach to have an impact in two ways on today's lighting practice.

First, we envision this method being used during the planning phase of a lighting installation (see Figure 12(a)). Image analysis could be integrated as a feature of a 3D rendering or lighting simulation software. To execute the analysis, the practitioner defines several views of interest. The software then visualizes the perceptual map for each view angle and provides a simple overview of the expected lighting outcome. Using our method, a perceptual analysis for the model could be completed within seconds. Based on the analysis, the practitioner might decide to change the room setup, for example, the type of luminaire, luminaire light output, and wall colour, and observe how these changes contribute to the visual experience. The practitioner might also compare the computed perceptual map with a target template to identify where changes are needed to achieve the wanted result.

The analysis could be used to optimize the layout and lighting scenes in a way that produces the largest perceptual difference between scenes to ensure a rich and interesting experience. For example in Experiment 2, Scenes 1, 3 and 6 are located very close to each other in the derived maps for one person offices (see Figure 11(1)–(6)). This indicates that their lighting effects are similar and that the setup or lighting configuration could be improved for these lighting scenes. Light output in Scene 6 could be lowered to increase perceptual difference between Scenes 3 and 1, which would alter the perceptual map to become more similar to the Lighting Lab, as shown in Figure 2.

For the second application, we envision this method being applied after the installation or for system retrofit (see Figure 12(b)). In this case, several photographs are taken automatically while the lights are changed to different preset configurations. Using the photographs and image analysis, a perceptual control map is generated for the installation. The user can use this perceptual map as a lower-dimensional control interface and more easily configure the lighting system, similar to the experiential controller introduced by Aldrich.[4] The user could also use the perceptual map to interface with context-aware applications, for example, to automate the lighting changes based on outputs of a wearable health monitor or other sensors in the home, smart home agents or security cameras,

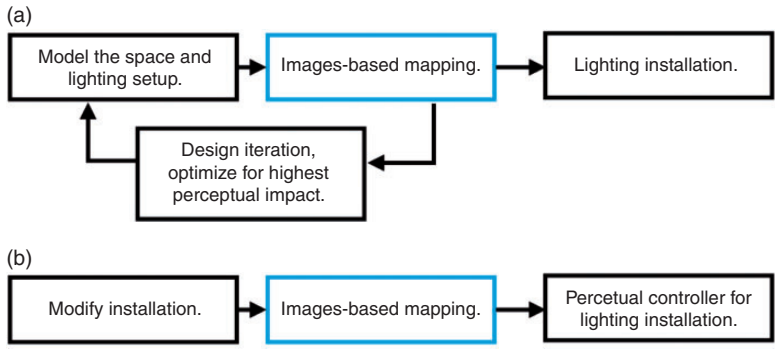

Figure 12 Workflow with perceptual analysis (a) during the planning phase and (b) after installation

similar to the implementation created by Zhao *et al.*[9]

The lower dimensional representation derived from images requires a linear transformation (e.g. translation and orthogonal rotation) to align with the rating-based maps or some general axes that would ensure a consistant orientation. It is not always required to give the perceptual map a reference. For example, we do not need a reference to maximize the perceptual difference of lighting scenes. However, if we wish to add a reference, normally the rating-based map of the space would not be available for the transformation. We envision three ways to acquire the transformation without the rating-based map.

The first possibility is to collect additional data through user ratings. The required human input is reduced because the distances between landmark scenes can be established through image-based mapping. As little as three coordinates would be sufficient to transform the two-dimensional map. If six lighting scenes are used, data could be theoretically collected for three instead of six lighting scenes, which would reduce the amount of human input to half.

The second possibility is to use the rating-based map generated from our experiment as a template for the linear transformation. The simulation study revealed that a general pattern was present in all 2D representations, despite differences in room size, the layout of the lighting system, furniture, scene configurations, etc. In particular, the dissimilarity was the lowest between variations of the same type of office. The commonalities among the simulated spaces were the kind of luminaires and the basic arrangement pattern, e.g. the distance between wall washing luminaires, and a few fundamental attributes of the scenes. Within these constraints, a template could be used to transform the image-based map. Such templates could be created for each type of space. Our current rating-based map appears to be most suitable for a small office.

The third option is to use machine learning on a large set of space- and perception data. Our current results are encouraging for this option because we were able to see prominent features in the image data.

10. Conclusion

This paper introduced image-based mapping, an approach that allows a user or practitioner to rapidly evaluate the perceptual impression of lighting scenes using images of the lit environment. We extracted dissimilarity information from photographs and simulated renderings of the lit environment and visualized them in a perceptual map. In an experiment to evaluate this method, we found that we were able to closely approximate human perceptual ratings (normalized dissimilarity value <0.04).

The comparison revealed that PCA is the most suitable algorithm for image-based mapping for our choice of landmark lighting scenes. The comparison of parameters confirmed that the latent structure can be discovered on basis of the distant samples, which were the landmark lighting scenes. A very low image resolution, e.g. 6 by 6 pixels can be sufficient for the analysis of lighting scenes with large uniform luminance surfaces. However, to ensure a relevant result, a higher resolution should be used for spaces with local contrast. We identified the exposure as the most impacting parameter; therefore, this parameter needs to be set with care according to the design.

To study the generalisability of the perceptual control map, we compared different office types using simulation and discovered high similarities among the maps for different variations of spaces. Room size had the most significant effect, whereas furniture and a diffusely lit window generated less distinct results. This outcome led us to conclude that

the perceptual map can be generalized for the same type of spaces if the lighting installation and scenes are constrained. We discussed three methods to generalize the perceptual control map using image-based mapping. Possible applications based on these findings are the computational analysis of visual impact during the planning phase and automated calibration for lighting control.

Declaration of conflicting interests

The authors declared no potential conflicts of interest with respect to the research, authorship, and/or publication of this article.

Funding

The authors received no financial support for the research, authorship, and/or publication of this article.

Acknowledgements

We want to thank Steelcase, Nathaniel Jones, and Yoav Reches for their support on generating the image datasets.

References

1 Figueiro MG, Brainard GC, Lockley SW, Revell VL, White R. *Light and Human Health*: *An Overview of the Impact of Optical Radiation on Visual, Circadian, Neuroendocrine, and Neurobehavioral Responses*. IES TM-18-08. New York: Illuminating Engineering Society of North America, 2008.
2 Mott MS, Robinson DH, Walden A, Burnette J, Rutherford AS. Illuminating the effects of dynamic lighting on student learning. *Sage Open* 2012; 2: 1–9.
3 Veitch JA. Psychological processes influencing lighting quality. *Journal of the Illuminating Engineering Society* 2001; 30: 124–140.
4 Aldrich MM. *Experiential lighting*: *development and validation of perception-based lighting controls*. Doctoral dissertation. Cambridge: Massachusetts Institute of Technology, 2014.
5 Ross P, Keyson DV. The case of sculpting atmospheres: towards design principles for expressive tangible interaction in control of ambient systems. *Personal and Ubiquitous Computing* 2007; 11: 69–79.
6 Magielse R, Ross PR. *A design approach to socially adaptive lighting environments*: *Proceedings of the 9th ACM SIGCHI Italian Chapter International Conference on Computer-Human Interaction*: *Facing Complexity*, Alghero, Italy, 13–16 September 2011, pp. 171–176.
7 Flynn JE, Spencer TJ, Martyniuk O, Hendrick C. Interim study of procedures for investigating the effect of light on impression and behavior. *Journal of the Illuminating Engineering Society* 1973; 3: 87–94.
8 Newsham G, Veitch J, Arsenault C, Duval C. *Effect of dimming control on office worker satisfaction and performance*: *Proceedings of the IESNA Annual Conference*, Tampa, FL, 25–28 July 2004, pp. 19–41.
9 Zhao N, Aldrich M, Reinhart CF, Paradiso JA. *A multidimensional continuous contextual lighting control system using Google glass*: *Proceedings of the 2nd ACM International Conference on Embedded Systems for Energy-Efficient Built Environments*, Seoul, South Korea, 4–5 November 2015, pp. 235–244.
10 Tan F, Caicedo D, Pandharipande A, Zuniga M. Sensor-driven, human-in-the-loop lighting control. *Lighting Research and Technology*. Epub ahead of print 21 February 2017. DOI: 10.1177/1477153517693887.
11 Newsham GR, Arsenault C. A camera as a sensor for lighting and shading control. *Lighting Research and Technology* 2009; 41: 143–163.
12 Inanici MN. Evaluation of high dynamic range photography as a luminance data acquisition system. *Lighting Research and Technology* 2006; 38: 123–134.
13 Villa C, Labayrade R. Multi-objective optimisation of lighting installations taking into account user preferences – a pilot study. *Lighting Research and Technology* 2013; 45: 176–196.

14 Inanici M. Evalution of high dynamic range image-based sky models in lighting simulation. *Leukos* 2010; 7: 69–84.
15 Newsham GR, Cetegen D, Veitch JA, Whitehead L. Comparing lighting quality evaluations of real scenes with those from high dynamic range and conventional images. *ACM Transactions on Applied Perception* 2010; 7: 13.
16 Jones NL, Reinhart CF. *Validation of GPU lighting simulation in naturally and artificially lit spaces*: *Proceedings of BS2015*: *14th Conference of the International Building Performance Simulation Association*, Hyderabad, India, 7–9 December 2015, pp. 1229–1236.
17 Wang HH, Luo MR, Liu P, Yang Y, Zheng Z, Liu X. A study of atmosphere perception of dynamic coloured light. *Lighting Research and Technology* 2014; 46: 661–675.
18 Whitman BA. *Learning the meaning of music*. Doctoral dissertation. Cambridge: Massachusetts Institute of Technology, 2005.
19 Spotify. *Spotify: music for everyone*. Retrieved 1 August 2017, from https:// www.spotify. com/.
20 Shacked R, Lischinski D. Automatic lighting design using a perceptual quality metric. *Computer Graphics Forum* 2001; 20: 215–227.
21 Anrys F, Dutré P, Willems YD. *Image-based lighting design*: *Proceedings of the 4th IASTED International Conference on Visualization, Imaging, and Image Processing*, Marbella, Spain, 6–8 September 2004, p. 15.
22 Ward G, Simmons M. JPEG-HDR: A backwards-compatible, high dynamic range extension to JPEG: *ACM SIGGRAPH 2006 Courses*, July 3: 2006.
23 Fechner GT. *Elemente der Psychophysik*. Vol. Vol. 2, Leipzig, Germany: Breitkopf and Hartel, 1907.
24 Van der Maaten LPJ. *An Introduction to Dimensionality Reduction Using Matlab*. Report. Maastricht, the Netherlands: University of Maastricht, 2007.
25 Kendall DG. A survey of the statistical theory of shape. *Statistical Science* 1989; 4: 87–99.
26 Team RC. *R Language Definition*. Vienna: R Foundation for Statistical Computing, 2000.
27 Kaiser HF. The varimax criterion for analytic rotation in factor analysis. *Psychometrika* 1958; 23: 187–200.
28 Magic Lantern. *Magic lantern for canon*. Retrieved 1 August 2017, from www. magiclantern.fm/.
29 Ward G. *Anywhere*. Retrieved 1 August 2017 from, www.anyhere. com/.
30 Jones NL, Reinhart CF. Experimental validation of ray tracing as a means of image-based visual discomfort prediction. *Building and Environment* 2017; 113: 131–150.
31 Van der Maaten L, Postma E, Van den Herik J. Dimensionality reduction: a comparative review. *Journal of Machine Learning Research* 2009; 10: 66–71.
32 Maaten LV, Hinton G. Visualizing data using t-SNE. *Journal of Machine Learning Research* 2008; 9: 2579–2605.
33 MathWorks. MATLAB single camera calibration app. Retrieved 1 August 2017, from www.mathworks.com/help/vision/ ug/single-camera-calibrator-app.html.
34 Ward GJ. *The RADIANCE lighting simulation and rendering system*: *Proceedings of the 21st Annual Conference on Computer Graphics and Interactive Techniques*, Orlando, FL, 24–29 July 1994, pp. 459–472.
35 KeyShot. *KeyShot 6*. Retrieved 1 August 2017, from www.keyshot.com/.
36 Santamaría-Peña J, Benito-Martín MA, Sanz-Adán F, Arancón D, Martinez-Calvo MA. Reliable low-cost alternative for modeling and rendering 3D objects in engineering graphics education. In: *Advances on Mechanics, Design Engineering and Manufacturing*. Cham: Springer, 2017: 923–930.